AU during an apparent outburst. S. J. Bus, M. F. A'Hearn, D. G. Schleicher, E. Bowell, *Science* **251**, 774 (1991).

5. Previously, the most distant detection of cometary CN emission was in the coma of P/Halley at r_h of 4.7 AU in February and March of 1985. S. Wyckoff, R. M. Wagner, P. A. Wehinger, D. G. Schleicher, M. C. Festou, *Nature* **316**, 241 (1985).
6. The Multiple Mirror Telescope Observatory, is a joint facility of the University of Arizona and the Smithsonian Institution. The spectra covered 3200 to 6700 Å at a dispersion of 1.2 Å pixel^{-1} and when combined with a 1-arc-sec-wide entrance slit our spectral resolution was 3.6 Å full-width at half-maximum (FWHM). The scale in the spatial direction was 0.6″ pixel^{-1} or 2890 km pixel^{-1} at the comet. Due to other programs, the total length of the slit was constrained to be 75 arc sec or 3.6×10^5 km at the comet. Image motion tests at the end of the night through one telescope indicated that the seeing was 0.9-arc-sec FWHM. However, the combined beam of the ensemble of telescopes and spectrograph optics yielded stellar images 2 to 3 arc sec FWHM and 6 to 7 arc sec full-width at zero intensity so there was loss of light from the standard calibration stars through the 1-arc-sec-wide slit. The transparency of the sky was excellent during our observations.
7. R. M. Wagner, in *Astronomical CCD Observing and Reduction Techniques*, S. B. Howell, Ed., *Astron. Soc. Pac. Conference Series* **23**, 160 (1992).
8. R. M. Wagner, B. L. Lutz, S. Wyckoff, *Astrophys. J.* **322**, 544 (1987).
9. D. G. Schleicher, thesis, University of Maryland (1983).
10. M. F. A'Hearn, R. L. Millis, D. G. Schleicher, D. J. Osip, P. V. Birch, *Icarus* **118**, 223 (1995).
11. C. E. Randall, D. G. Schleicher, R. G. Rallou, D. J. Osip, *Bull. Am. Astron. Soc.* **24**, 1002 (1992); C. E. Randall and D. G. Schleicher, in preparation.
12. D. G. Schleicher, S. M. Lederer, R. L. Millis, T. L. Farnham, *Science* **275**, 1913 (1997).
13. M. Kleine, S. Wyckoff, P. A. Wehinger, B. A. Peterson, *Astrophys. J.* **436**, 885 (1994).
14. A. L. Cochran, *Bull. Am. Astron. Soc.* **28**, 1093 (1996); private communication.
15. The reflectance spectrum was derived by dividing the spectrum of the comet by the spectrum of the solar analog star and then normalized to unity at 5500 Å.
16. We thank the staff of the Multiple Mirror Telescope Observatory for their efforts which made these observations possible. This work was partially supported by NASA grants NAG5-2355 to The Ohio State University and NAGW-3884 to Lowell Observatory.

10 February 1997; accepted 6 March 1997

Diffusing-Wave Spectroscopy of Dynamics in a Three-Dimensional Granular Flow

Narayanan Menon and Douglas J. Durian

Diffusing-wave spectroscopy was used to measure the microscopic dynamics of grains in the interior of a three-dimensional flow of sand. The correlation functions show that minutely separated grains fly from collision to collision with large random velocities. On a time scale 10^3 to 10^4 times longer than the average time between collisions, the grains displayed slow, collective rearrangements, which, at the long-time limit, produced diffusive dynamics.

Sand dunes, grain silos, hourglasses, catalytic beds, filtration towers, river beds, ice fields, and many foods and building materials are granular systems (*1*). They consist of large numbers of randomly arranged, distinct, macroscopic grains that are too large to be moved by thermal energies but can be driven into flow by external forces. We do not have an understanding of the fluid state of a granular medium analogous to that for the macroscopic flow properties of a liquid. In a series of seminal papers, Bagnold (*2*) made the first efforts toward creating a phenomenological "fluid mechanics" for sand, identifying inertia of the grains and their collisions as significant elements in the dynamics. Since then there has been considerable theoretical effort (*3*) in formulating a continuum description of granular flows based on the kinetic theory of dense gases. However, in contrast to molecular fluids, kinetic energy in grain flows is irreversibly lost in the inelastic collisions of the grains. A further complication is that the scale of velocity fluctuations in the material (referred to as the "granular temperature") is nonthermal and has been difficult to measure, especially in three-dimensional (3D) flows (*4*). Also, recent computer simulations and theoretical work (*5*) show that 1D and 2D inelastic systems spontaneously form inhomogeneities that potentially restrict the applicability of hydrodynamic approaches to grain flow.

We used diffusing-wave spectroscopy (DWS) (*6*) to probe the local, short-time dynamics of grains in a 3D gravity-driven flow and examine the physical basis of hydrodynamic models. DWS is a multiple–light-scattering technique that yields two-particle correlation functions at time intervals greater than 10^{-8} s and spatial separations greater than 1 Å. These capabilities are necessary because the collisional dynamics we studied are at time scales of 10^{-6} to 10^{-4} s and length scales of 0.01 to 1 μm. Because granular materials strongly scatter light, earlier experiments have chiefly studied quasi-2D flows (*7*) or highly diluted flows (where the short-time dynamics are collisional by construction). Experiments in dense flows (*8–10*) have been analyzed (*8*, *9*) with the assumptions that short-time dynamics are collisional and that the quantities of interest may be inferred from long-time, spatially averaged motions obtained by direct imaging of tracer beads.

The granular material we studied consisted of dry, cohesionless, monodisperse, smooth, spherical glass beads (*11*) 95 or 194 μm in diameter. The flow was gravity-driven (*12*) and confined to a vertical channel 30 cm high, 10 cm wide, and 0.3 to 1 cm thick (Fig. 1). Video and DWS measurements showed that spatial gradients in all three dimensions were small and that the flow field everywhere in the channel was characterized by a single average flow velocity V_f. We varied V_f from 0.03 to 3 cm/s by changing the mesh size at the bottom of the channel. The arrangement of the beads in flow showed no evidence of density inhomogeneities or crystalline packing.

For DWS measurements, we illuminated the sample with an Ar^+ laser of 488- or 514-nm wavelength and 3-mm beam waist. Incident photons were multiply scattered by the glass beads, performed random walks through the sample, and interfered, producing a speckled pattern. Grain motions caused this pattern to fluctuate, decorrelating the intensity measured at the detector. To infer the dependence of the dynamics of the beads on time τ from the autocorrelation function $g_1(\tau)$, we described photon transport as a random walk through the medium with a step length l^* and an absorption length l_A (which were determined by measuring the fraction of light transmitted through the sample as a function of its thickness). For example, the normalized electric-field autocorrelation function in transmission (Fig. 2A) is $g_1(\tau) \approx \exp[-(L/l^*)^2 k^2 \langle \Delta r^2(\tau) \rangle]$, where L is the sample thickness, $\langle \Delta r^2(\tau) \rangle$ is the mean-squared displacement of the scatterers, k is the wave vector of light in the medium, and the factor $(L/$

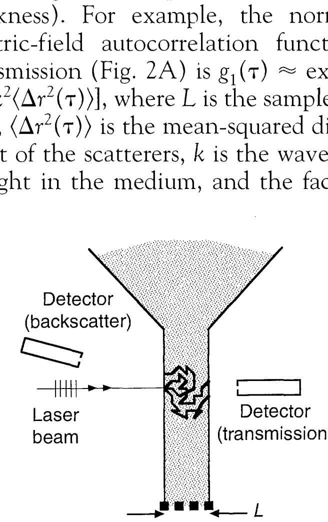

Fig. 1. Side view of the flow and light-scattering geometry.

Department of Physics and Astronomy, University of California, Los Angeles, CA 90095–1547, USA.

$l^*)^2$ represents the number of random steps of length l^* in an average photon path. The complete solution of the photon diffusion equation with boundary conditions—specified by the geometry of the sample, the illuminating beam, and the detection optics—is weighted by paths of all lengths and includes absorption effects (6).

In such an inversion, the curves for $\langle \Delta r^2(\tau) \rangle$ from backscattering and transmission coincided (Fig. 2B) even though they were derived from markedly different $g_1(\tau)$, which shows that the analysis was reliable. Furthermore, this result implies that the dynamics of grains are uniform across the thickness of the channel, because $g_1(\tau)$ samples very different distributions of photon paths in these two scattering geometries: Photons transmitted through the sample were scattered by grains through the bulk of the sample, whereas photons backscattered from the sample were scattered mainly within a few l^* of the illuminated wall. The result in Fig. 2, B and C, demonstrates that the motion of sand grains at short times was ballistic, that is, $\langle \Delta r^2(\tau) \rangle = (\delta V)^2 \tau^2$, where δV is a randomly directed velocity. Each grain remained in free flight for a mean free time τ_c until a collision with a neighboring grain randomized the direction of the next ballistic flight. From δV and τ_c, we can determine the mean free path $s = \delta V \tau_c$, corresponding to the average distance between the surfaces of neighboring grains. Repeated collisions eventually changed the relative positions of grains. This movement was reflected in the slow increase in $\langle \Delta r^2(\tau) \rangle$ at times longer than τ_c. This interpretation of $\langle \Delta r^2(\tau) \rangle$ as a single-particle quantity is independent of spatial correlations between beads because in $g_1(\tau)$ the structure factor is weighted heavily to large scattering wave vectors (13). These features in the signal only reflect relative motions of beads; the effect of the average downward drift of beads was to continuously change the set of beads being sampled and contributed to the decay of $g_1(\tau)$ at a longer time scale (estimated by $D/V_f \approx 0.1$ to 10 s, where D is the beam waist).

The data in Fig. 2B show that the dynamics of grains are dominated by collisions rather than sliding contacts, even in dense, slow flows. The average velocity fluctuations were large ($\delta V \approx 0.31$ cm/s) and comparable to the overall flow velocity ($V_f \approx 0.32$ cm/s). The collisional frequency was high, and the interparticle separation was small: For the data in Fig. 2B, the average collision time and distance were $\tau_c \approx 9$ μs and $s \approx 0.028$ μm, respectively. Our data show that the dilation of sand in flow (14) may be tiny compared to the particle diameter d ($s/d \approx 10^{-4}$). Thus, although the bulk density of the sand may be almost unchanged by flow, the relative motions of the particles reflect a state of great activity. Our measurement establishes that there can be a "granular temperature" in the absence of a shear gradient. This result contradicts hydrodynamic models (15), which find $\delta V \rightarrow 0$ in this geometry, except in a shear layer at the boundary. Our experiment, however, does not establish that $(\delta V)^2$ has all the attributes of a temperature; in particular, we do not know if the velocity fluctuations are isotropic and Boltzmann-distributed. However, because the short-time limit of $\langle \Delta r^2(\tau) \rangle / \tau^2 = (\delta V)^2$ is well defined, the distribution at large velocities is stronger than a power law, which is consistent with a Boltzmann distribution.

We measured the dependencies of each of these microscopic quantities—δV, τ_c, and s—on V_f. The mean velocity fluctuation δV was the same order of magnitude as V_f for the range covered in this experiment (Fig. 3A). The data can be approximated by a power law: $\delta V \propto V_f^{2/3}$ over this range. The origin of this power law and its exponent are unknown. The mean collision time τ_c showed only a weak dependence on V_f (Fig. 3B). The collision frequency ranged from about 500 kHz (for d = 95 μm) to 10 kHz (for d = 194 μm). From τ_c and δV, we obtained s (Fig. 3C). The dilation ranged from 0.01 to 0.1% of the sphere diameter.

These data (Fig. 3) are consistent with energy and momentum balance for typical values of the coefficient of restitution e for glass spheres. For example, even the small dilation in Fig. 3C is sufficient for gravity to produce the large random velocities measured. However, energy and momentum budgets do not fully capture the dependence of the measured parameters on the driving velocity V_f. An energy balance between gravitational energy gained and kinetic energy lost because of inelasticity gives $(1 - e^2)[m(\delta V)^2/2]/\tau_c \sim mgV_f$, where m is the particle mass and g is acceleration due to gravity. Likewise, if we assume that the velocities of neighboring grains are uncorrelated and that collisions completely decorrelate velocity autocorrelations, we obtain an estimate $em\delta V \propto mg\tau_c$. Together, these give a scaling $\delta V \propto V_f$, which differs from the experimental scaling. A treatment of particle motions as uncorrelated thus seems

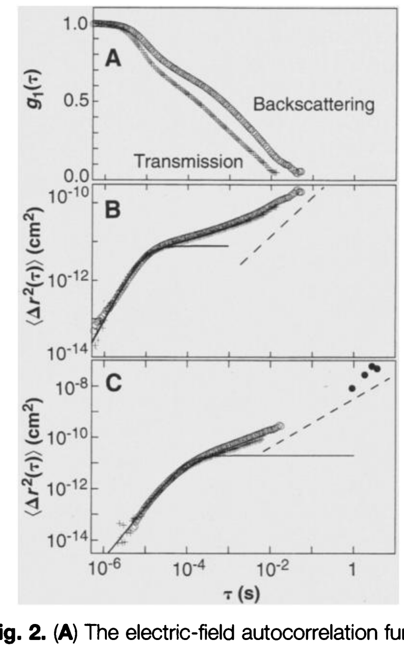

Fig. 2. (**A**) The electric-field autocorrelation function $g_1(\tau)$ for transmission (+) and backscattering (O) [obtained from the intensity autocorrelation function using the Siegert relation (18)] for 95-μm sand with l^*/d = 7.5 and l_A/l^* = 17. (**B**) $\langle \Delta r^2(\tau) \rangle$ versus τ for 95-μm sand. (**C**) $\langle \Delta r^2(\tau) \rangle$ versus τ for 194-μm sand. The solid lines are fits to the form $(\delta V \tau)^2/[1 + (\tau/\tau_c)^2]$, which represents ballistic motion with a random velocity δV within a cage of size $\delta V \tau_c$. There was subdiffusive motion over several decades in time for $\tau > \tau_c$ that became diffusive (dashed line) in the long-time limit, as shown by video measurements (●) of single-particle diffusion in one dimension perpendicular to the flow.

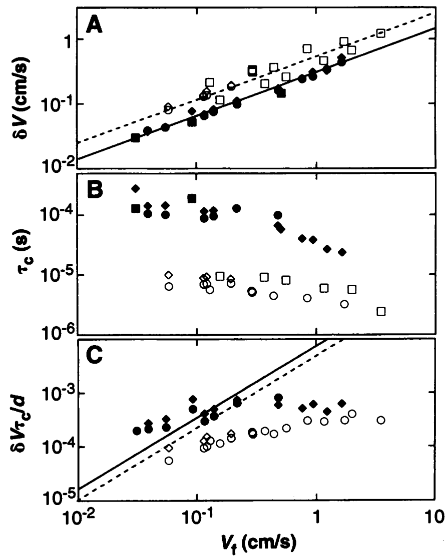

Fig. 3. Microscopic scales of motion versus macroscopic flow velocity V_f. (**A**) Mean velocity fluctuation δV versus V_f. The lines are power-law fits (with an exponent of ⅔) to the 95-μm (dashed line and open symbols) and 194-μm (solid line and filled symbols) data. (**B**) Mean collision time τ_c versus V_f. (**C**) Mean free path $s = \delta V \tau_c$, scaled to the particle diameter d. The lines show $(\delta V)^2/2gd$, the fraction of its own diameter a particle must fall under the influence of gravity to attain a speed δV. The conformity of measurements in various flow geometries [cells with L = 0.32 cm (open squares), 0.625 cm (circles), and 0.92 cm (filled squares)] and various scattering geometries [transmission (squares and circles) and backscattering (diamonds)] indicates that spatial gradients perpendicular to the walls of the channel were small enough that all measured quantities are functions of only V_f (19).

insufficient, suggesting that collective effects, such as velocity correlations between particles (*16*) or slowly decaying velocity autocorrelations, may be important.

All of the features in Fig. 3 refer to motions at times less than τ_c. At times longer than τ_c, the relative displacement of grains is characterized by subdiffusive motion, which presumably corresponds to gradual rearrangements of neighboring grains, over several orders of magnitude in time (Fig. 2, B and C). We did not obtain the diffusive limit $\langle \Delta r^2(\tau) \rangle \propto \tau$, even at the end of the range available to DWS. Measurements by long-range video microscopy (solid circles in Fig. 2C) show that relative motions of sand grains in the direction transverse to V_f ($\hat{y}$) and in the plane of the channel were diffusive (*17*). The time for rearrangement of nearest neighbors was 0.1 to 10 s, so that if relative motion is diffusive, it is a consequence of complex collective behavior. Hunt and others (*8*) reported experiments on video imaging of granular material in channel flow from which they extracted diffusion constants; similar experiments have been performed on vibrated granular systems (*9*). Our data indicate that the parameters of collisional dynamics cannot be deduced from such measurements using conventional prescriptions such as the Langevin equation as a bridge between short-time ballistic motion and long-time diffusion; for example, the diffusion coefficient of the grains in our experiment was much less than $s\delta V$.

The wide separation of time scales between collisional dynamics and the long-time diffusive limit suggest that complex collective dynamics occur even in the absence of long-wavelength clustering instabilities (*5*), reminiscent of dynamics in glassy systems such as viscous liquids and dense colloids. Our simple realization of a granular flow accentuates the contrast between a molecular fluid, where viscous loss occurs only in shear gradients, and sand, where a region of uniform flow dissipates energy because, as our results show, velocity fluctuations exist even in the absence of macroscopic gradients.

REFERENCES AND NOTES

1. H. M. Jaeger and S. R. Nagel, *Science* **255**, 1523 (1992); ______ and R. P. Behringer, *Phys. Today* **49**, 32 (April 1996); C. S. Campbell, *Annu. Rev. Fluid Mech.* **22**, 57 (1990).
2. R. A. Bagnold, *Proc. R. Soc. London Ser. A* **225**, 49 (1954); *ibid.* **295**, 219 (1966).
3. S. Ogawa, in *Proceedings of the U.S.–Japan Symposium on Continuum Mechanics and Statistical Approaches in the Mechanics of Granular Materials*, S. C. Cowin and M. Satake, Eds. (Gakujutsu Bunken Fukyukai, Tokyo, 1979), pp. 208–217; J. T. Jenkins and S. B. Savage, *J. Fluid Mech.* **130**, 187 (1983); P. K. Haff, *ibid.* **134**, 401 (1983); J. Schofield and I. Oppenheim, *Physica A* **196**, 209 (1993).
4. G. D. Cody, D. J. Goldfarb, G. V. Storch Jr., and A. N. Norris [*Powder Technol.* **87**, 211 (1996)] inferred velocity fluctuations in a fluidized bed from the acoustic response of the container to discrete collisions of particles.
5. M. A. Hopkins and M. Y. Louge, *Phys. Fluids A* **3**, 47 (1991); I. Goldhirsch and G. Zanetti, *Phys. Rev. Lett.* **70**, 1619 (1993); S. McNamara and W. Young, *Phys. Rev. E* **50**, R28 (1994); D. R. M. Williams and F. C. MacKintosh, *ibid.* **54**, R9 (1996).
6. G. Maret and P. E. Wolf, *Z. Phys. B* **65**, 409 (1987); D. J. Pine, D. A. Weitz, P. M. Chaikin, E. Herbolzheimer, *Phys. Rev. Lett.* **60**, 1134 (1988); D. J. Pine, D. A. Weitz, J. X. Zhu, E. Herbolzheimer, *J. Phys. (France)* **51**, 2101 (1990).
7. T. G. Drake, *J. Fluid Mech.* **225**, 121 (1991).
8. S. S. Hsiau and M. L. Hunt, *ibid.* **251**, 299 (1993); V. V. R. Natarajan, M. L. Hunt, E. D. Taylor, *ibid.* **304**, 1 (1995).
9. O. Zik and J. Stavans, *Europhys. Lett.* **16**, 255 (1991).
10. M. Nakagawa *et al.*, *Exp. Fluids* **16**, 54 (1993); E. E. Ehrichs *et al.*, *Science* **267**, 1632 (1995).
11. Jaygo (Union, NJ) and Cataphote (Jackson, MS).
12. The effect of the ambient air was small because the weight of the grains was at least 10^4 times the Stokes drag. Dissipation was primarily through inelastic collisions, which (for typical grain velocities and a coefficient of restitution of 0.9) was greater by a factor 10^4 than the energy lost to the viscous drag of the air.
13. S. Fraden and G. Maret, *Phys. Rev. Lett.* **65**, 512 (1990); X. Qiu *et al.*, *ibid.*, p. 516; J.-Z. Xue *et al.*, *ibid.* **69**, 1715 (1992).
14. O. Reynolds, *Philos. Mag.* **20**, 469 (1885).
15. K. Hui and P. K. Haff, *Int. J. Multiphase Flow* **12**, 189 (1986).
16. Y. H. Taguchi and H. Y. Takayasu, *Europhys. Lett.* **30**, 499 (1995).
17. These points are obtained from the width of $[\mathbf{r}(0) - \mathbf{r}(\tau)]\cdot\hat{\mathbf{y}}$ averaged over many particles and starting times. For comparison with the value of $\langle \Delta r^2(\tau) \rangle$ obtained from DWS, this quantity is multiplied by a factor of 3.
18. B. J. Berne and R. Pecora, *Dynamic Light Scattering: With Applications to Chemistry, Biology and Physics* (Wiley, New York, 1976).
19. We directly confirmed that the gradients in the other two directions were small by moving the beam across the channel.

5 August 1996; accepted 28 January 1997

Single-Electron Transport in Ropes of Carbon Nanotubes

Marc Bockrath, David H. Cobden, Paul L. McEuen,* Nasreen G. Chopra, A. Zettl, Andreas Thess, R. E. Smalley

The electrical properties of individual bundles, or "ropes," of single-walled carbon nanotubes have been measured. Below about 10 kelvin, the low-bias conductance was suppressed for voltages less than a few millivolts. In addition, dramatic peaks were observed in the conductance as a function of a gate voltage that modulated the number of electrons in the rope. These results are interpreted in terms of single-electron charging and resonant tunneling through the quantized energy levels of the nanotubes composing the rope.

In the past decade, transport measurements have emerged as a primary tool for exploring the properties of nanometer-scale structures. For example, studies of quantum dots have illustrated that single-electron charging and resonant tunneling through quantized energy levels regulate transport through small structures (*1*). Recently, much attention has been focused on carbon nanotubes (*2*). Their conducting properties are predicted to depend on the diameter and helicity of the tube, parameterized by a roll-up vector (n, m). One type of tube, the so-called (n, n) or armchair tube, is expected to be a one-dimensional (1D) conductor with current carried by a pair of 1D subbands (*3*) (Fig. 1, right inset). A recent breakthrough has made it possible to obtain large quantities of the (10, 10) single-walled nanotube (SWNT), which is ~1.4 nm in diameter (*4*). This advance, in combination with recent successes in performing electrical measurements on individual multi-walled nanotubes (MWNTs) (*5–7*) and nanotube bundles (*8*), makes possible the study of the electrical properties of this 1D system.

We have measured transport through bundles, or ropes, of nanotubes bridging contacts separated by 200 to 500 nm. A gap (suppressed conductance at low bias) is observed in the current-voltage (I-V) curves at low temperatures. Further, dramatic peaks are observed in the conductance as a function of a gate voltage V_g that modulates the charge per unit length of the tubes. These observations are consistent with single-electron transport through a segment of a single tube with a typical addition energy of ~10 meV and an average level spacing of ~3 meV.

The device geometry (Fig. 1, left inset) consists of a single nanotube rope to which

M. Bockrath, D. H. Cobden, P. L. McEuen, N. G. Chopra, A. Zettl, Molecular Design Institute, Lawrence Berkeley National Laboratory, and Department of Physics, University of California, Berkeley, CA 94720, USA.
A. Thess and R. E. Smalley, Center for Nanoscale Science and Technology, Rice Quantum Institute, and Departments of Chemistry and Physics, Mail Stop 100, Rice University, Post Office Box 1892, Houston, TX 77251, USA.

*To whom correspondence should be addressed.